Crystal Growth Rates of Paracetamol in Mixtures of Water + Acetone + Toluene

Roger A. Granberg and Åke C. Rasmuson
Dept. of Chemical Engineering and Technology, Royal Institute of Technology, SE-10044 Stockholm, Sweden

DOI 10.1002/aic.10512
Published online June 24, 2005 in Wiley InterScience (www.interscience.wiley.com).

Crystal growth rates of paracetamol (4-hydroxyacetanilide) have been determined by seeded isothermal desupersaturation experiments at 16 °C in 23 different solvent mixtures of water + acetone + toluene. Parameters of different growth rate equations have been estimated by direct nonlinear optimization. At equal thermodynamic driving force, the growth rate depends on the composition of the solvent mixture. In the surface diffusion spiral growth model, this dependency can be described in terms of the interfacial energy between the solid and the solution. A reasonable prediction of the influence of the solvent composition on this interfacial energy is obtained if a proper estimation of the enthalpy of dissolution is done. For the case of paracetamol crystals growing in water + acetone + toluene mixtures this estimation needs to include an estimation of the entropy of fusion at the temperature of growth as well as of the nonideal entropy of mixing. © 2005 American Institute of Chemical Engineers *AIChE J,* 51: 2441–2456, 2005
Keywords: crystallization, crystal growth, solvents, interfacial energy, puracetamol, chemical potential driving force

Introduction

The manufacture of organic fine chemicals, specialty chemicals, and pharmaceuticals often involves crystallization from organic solvents or mixtures of solvents. The composition of the solvent determines the solubility and thus influences the supersaturation. Furthermore, the solvent composition may influence the nucleation rate as well as the relative growth rate of each crystal face, and it may thus affect the shape of the product crystals and the size distribution of the entire crystallized mass. The solvent composition may also influence aggregation/agglomeration properties and the purity of the crystals. The solvent may influence crystal growth through its effect on solution properties (such as viscosity, density, or component diffusivities), on the structure of the crystal–liquid interface and on the solubility (Klug, 1993).

Concerning the growth rate of a particular face, Davey (1982) suggests two possible roles for the influence of solvent. The solvent may influence the growth mechanism by an influence on the surface roughness. Calculations suggest that the net effect of increasing solubility is that the growing surface becomes rougher, thus leading to a more rapid growth. This is supported by experimental results (Bourne and Davey, 1976; Duverneuil et al., 1987; Human et al., 1981; Olech and Hodorowicz, 1990; Skoda and Van den Tempel, 1967). However, specific adsorption of solvent molecules at the growing crystal surface can result in a lower growth rate despite a higher solubility, as has been experimentally observed for organic molecules with polar faces such as α-resorcinol (Davey et al., 1988) and succinic acid (Davey et al., 1982).

The influence of solvent composition on crystal growth rates has mainly been studied on single crystals (see, for example, Davey, 1982). There are very few studies in which the average particle growth rate has been determined in different solvents for a significant number of particles (mass crystallization). In the present work, overall crystal growth rates of paracetamol (PA) have been determined in 23 water + acetone + toluene mixtures at 16°C. In the experiments is a known amount of sieved seed crystals added to an isothermal supersaturated solution and the supersaturation decay is recorded (Bujac and Mullin, 1969; Jones

Correspondence concerning this article should be addressed to Å. C. Rasmuson at rasmuson@ket.kth.se.

and Mullin, 1973; Tanimoto et al., 1964). Growth kinetics are estimated by fitting a growth rate equation directly to the experimental desupersaturation curve, using nonlinear parameter estimation techniques (Qiu and Rasmuson, 1990).

Paracetamol is used as an intermediate in the manufacture of azo-dyes and photographic chemicals, and is characterized by antipyretic and analgesic properties. Previous studies on the crystallization of PA have concerned: solubility data (Granberg and Rasmuson, 1999, 2000); growth rate dispersion in aqueous solutions (Finnie et al., 1996, 1999); crystal habit modifications in water (Grant and Chow, 1991); the prediction of crystal morphology (Green and Meenan, 1996); the incorporation of impurities (Hendriksen et al., 1998); face growth kinetics (Shekunov et al., 1996, 1997); crystallization and agglomeration (Granberg et al., 1999); primary nucleation (Granberg et al., 2000); and agglomeration (Ålander and Rasmuson, 2003; Ålander et al., 2004; Uusi-Penttilä and Rasmuson, 2003). The solvent system water + acetone + toluene spans a large range of polarity where water, of course, is very polar, acetone is mildly polar, and toluene is nonpolar. Furthermore, the solvents are of industrial relevance.

Theory

Crystal growth in solution proceeds by diffusional mass transfer through the boundary layer surrounding the crystal, followed by surface integration. The surface integration involves desolvation, surface diffusion over the crystal surface, and sequential addition of growth units into the crystal lattice at favorable locations.

Face growth models

The integration of new molecules into the crystal lattice is quite unfavorable on a surface that is atomically smooth. At a molecular step or a kink (corner), integration is more favorable because binding can be established in more than one direction. Thus, the rate of surface integration depends on the presence of steps and kinks, that is, on the surface roughness. The roughness of the surface is described by the Jackson alpha factor, α, and three growth regimes have been identified (Davey, 1982).

If $\alpha > 5$, the surface is smooth and the attachment of new molecules is slow (slow growth regime). A reasonable growth rate is obtained only if there is a mechanism that generates dislocations on the surface. The spiral growth mechanism, as proposed in 1951 by Burton, Cabrera, and Frank (hereafter, the BCF model; Ohara and Reid, 1973) provides for the existence of nonvanishing dislocations, as described by

$$G_{hkl} = A_{\mathrm{BCF}}(S-1)\ln S \tan h\left(\frac{B_{\mathrm{BCF}}}{\ln S}\right) \tag{1a}$$

where

$$A_{\mathrm{BCF}} = \frac{2kTD_{\mathrm{S}}C_{\mathrm{SE}}\beta\gamma_o}{19\gamma_{sl}x_{\mathrm{S}}} \tag{1b}$$

$$B_{\mathrm{BCF}} = \frac{19V_m\gamma_{sl}}{2kTx_{\mathrm{S}}} \tag{1c}$$

where G_{hkl} is the rate of face growth in a direction perpendicular to the surface itself. The magnitude is mainly determined by A_{BCF}, whereas B_{BCF} determines the shape of the dependency on the supersaturation. At low supersaturation, when $\ln S \ll B_{\mathrm{BCF}}$, a parabolic law is obtained and Eq. 1a reduces to

$$G_{hkl} = A_{\mathrm{BCF}}(S-1)\ln S \tag{2}$$

When $3 < \alpha < 5$, the surface possesses a certain degree of roughness (intermediate growth regime), although the rate of growth is limited by the creation of new steps by two-dimensional (2D) nucleation on the face. The most favored model is the birth and spread (B+S) theory (Ohara and Reid, 1973):

$$G_{hkl} = A_{\mathrm{B+S}}(S-1)^{2/3}(\ln S)^{1/6}\exp\left(\frac{-B_{\mathrm{B+S}}}{\ln S}\right) \tag{3a}$$

where

$$A_{\mathrm{B+S}} = 2h^{1/6}V_m^{5/6}\left(\frac{\bar{v}}{\pi}\right)^{1/3}\left(\frac{n_1D_{\mathrm{S}}C_{\mathrm{SE}}\beta\gamma_o}{x_{\mathrm{S}}}\right)^{2/3} \tag{3b}$$

$$B_{\mathrm{B+S}} = \frac{\pi h V_{\mathrm{m}}\gamma_{sl}^2}{k^2T^2} \tag{3c}$$

If $\alpha < 3$ the surface is rough. Integration may take place almost at the location of arrival to the surface and the resistance to surface integration is low (Davey, 1982).

In the BCF and the B+S models, we assume that the influence of the solvent composition on the rate of growth is predominantly exerted by the influence on the solid–liquid interfacial energy (γ_{sl}). The effect of other quantities are, in practice, not readily separable from each other (Mersmann, 1995), and as a first approximation we assume the corresponding groups to be constant. In the B+S model the critical radius (r^*) of the 2D surface nucleus can be expressed as: $r^* = \gamma_{sl}V_m/\Delta\mu$ (Myerson and Ginde, 1993). The lower the interfacial energy, the smaller is the radius of the nuclei required for it to be stable, and thus the rate of nucleation increases. In the BCF model, the spiral creates a series of growth steps on the surface. The density of these steps is determined by the radius of the spiral center, which is assumed to be equal to the radius of a corresponding 2D nucleus (Bennema and Gilmer, 1973). In later developments kinks in the growth steps are also accounted for. At lower interfacial energy, there is a higher density of steps on the surface and a higher density of kinks in the step. Thus, the growth units need to diffuse a shorter distance before actual integration into the lattice takes place.

Interfacial energy and surface structure

The interfacial energy is the thermodynamic work required in forming a new interfacial area (Stokes and Evans, 1997) and is a direct manifestation of the unbalanced intermolecular forces of the molecules at the surface of the solid (Van Krevelen, 1990). The molecules at the surface possess additional free energy, in comparison to the corresponding molecules inside the solid, by an amount that is equal to the missing

contributions to its bonding. The magnitude of the interfacial energy of a crystal face depends on the crystal structure (coordination number), the bond character (strength of broken bond), and the orientation of the surface plane (density of broken bonds), and thus the interfacial energy differs for different faces. In addition, the energy associated with each surface site differs because the coordination number differs, and thus the interfacial energy depends on the surface roughness. Usually the interfacial energy between a solid and a liquid approaches zero as the affinity between the solute and the liquid-phase molecules increases.

The interfacial energy of a solid cannot be easily measured (Linford, 1972; Neumann and Spelt, 1996), although it can be estimated indirectly from induction time measurements (Söhnel and Mullin, 1988). Nielsen and Söhnel (1971) showed for inorganic compounds in aqueous solutions that the interfacial energy is a linear function of the logarithm of the solubility. This relationship was confirmed based on regular solution theory (Bennema and Söhnel, 1990), and somewhat modified in a thermodynamic approach by Mersmann (1990). We have found that this approach may predict values that are one order of magnitude too high for organic compounds (Granberg et al., 2000).

On qualitative grounds, Davey (1982) proposed that the interfacial energy should be proportional to the enthalpy of dissolution ΔH^{diss}. Bennema and Söhnel (1990) gave this approach a quantitative description:

$$\gamma_{sl} = \xi_\gamma \frac{\Delta H^{\text{diss}}}{N_A V_m^{2/3}} \tag{4}$$

expressed in molar units for a cubic growth unit. The interfacial energy is assumed to be that fraction (ξ_γ) of the enthalpy of dissolution that corresponds to the fraction of bonds that are not satisfied by the crystalline lattice. It is often assumed, in the estimation of the value of ξ_γ, that the solid–liquid bond energies at the surface are equal to those out in the solution, the equivalent wetting condition. ξ_γ ranges from 0.1 to 0.5, and in the correlation of experimental interfacial energy data $\xi_\gamma = 0.25$ was the best value (Bennema and Söhnel, 1990).

The α-factor (Jackson, 1958), defined as the fraction of all possible sites on the surface that are growth steps, appears in the equation describing the free energy change when atoms are added randomly to a surface. Extended to a generalized fluid/crystal interface model (Temkin, 1966) and by assuming complete wetting of the solid, the binding energy can be replaced by a fraction (ξ_α) of the enthalpy of dissolution (Bennema and Gilmer, 1973), expressed as

$$\alpha = \xi_\alpha \frac{\Delta H^{\text{diss}}}{RT} \tag{5}$$

The anisotropy factor ξ_α is usually between 0.5 and 1 for low index planes (Sloan and McGhie, 1988) and can be estimated by (Bennema, 1993)

$$\xi_\alpha = \frac{E^{\text{latt}} - E_{hkl}^{\text{att}}}{E^{\text{latt}}} \tag{6}$$

where E^{latt} is the lattice energy, which is independent of the crystallographic face (Hartman and Perdok, 1955), and E_{hkl}^{att} is the attachment energy, both of which can be estimated by molecular simulation using CERIUS^2.

Enthalpy of dissolution

Based on classical thermodynamics Jetten et al. (1984) defined a route to estimate the enthalpy of dissolution. At equilibrium between the solid and the melt (that is, at T_m) and between the solid and the saturated solution (at T), respectively, the Gibbs free energy for transformation of molecules from the solid state into the liquid is zero. Thus

$$\Delta H^{\text{diss}} = T\Delta S^{\text{diss}} \tag{7}$$

and

$$\Delta S_m^f = \Delta H_m^f / T_m \tag{8}$$

The process of dissolution (at T) is then assumed to be equal to the melting (ΔS^f) of the solute at T, followed by mixing (ΔS^{mix}) with an excess of nearly saturated solution:

$$\Delta S^{\text{diss}} = \Delta S^f + \Delta S^{\text{mix}} \tag{9}$$

The entropy of fusion at T is estimated through a thermodynamic pathway where the solid is heated from T to the melting point, is melted, and the melt is cooled down to T. Thus, the entropy change upon melting at T becomes

$$\Delta S^f = \int_T^{T_m} \frac{C_{p,s}}{T}\, dT + \Delta S_m^f + \int_{T_m}^{T} \frac{C_{p,l}}{T}\, dT \tag{10}$$

where $C_{p,l}$ and $C_{p,s}$ are the heat capacities for the supercooled melt and the solid, respectively.

The entropy of mixing was determined by assuming a regular solution, for which the entropy of mixing equals that of an ideal solution:

$$\Delta S^{\text{mix}} = \Delta S^{\text{ideal}} = -R \ln x_{eq}(T) \tag{11}$$

Using Eqs. 7–11 leads to

$$\begin{aligned}\Delta H^{\text{diss}} &= T(\Delta S^f + \Delta S^{mix}) \\ &= T\left(\Delta S_m^f - \int_T^{T_m} \frac{\Delta C_p}{T}\, dT - R \ln x_{eq}(T)\right)\end{aligned} \tag{12}$$

where

$$\Delta C_p = C_{p,l} - C_{p,s} \tag{13}$$

The first two terms on the right-hand side of Eq. 12 estimate the entropy of fusion at temperature T, which is independent of the solvent. As long as the solid phase is pure, it depends on the

Table 1. Chemicals Used in Experimental Work

Compound	Water Content	Residue after Evaporating	Supplier
Paracetamol	<0.1%*	—	Astra Production Chemicals, Sweden
Acetone	0.03%	<0.001%	Merck, Germany
Toluene	0.01%	<0.001%	Merck, Germany

*The value is the loss on drying at 105°C, which includes all volatile compounds.

solute only. The third term on the right-hand side contains all the dependency on the solvent composition.

Experimental Work

In the present work, overall crystal growth rates of paracetamol have been determined in 23 binary and ternary mixtures of water + acetone + toluene at 16°C. In the experiments is a known amount of sieved seed crystals added to an isothermal supersaturated solution. As the crystals grow, the supersaturation decay is recorded. Growth kinetics are estimated by fitting a growth rate equation directly to the experimental desupersaturation data, using nonlinear parameter estimation techniques (Qiu and Rasmuson, 1990).

Materials

Acetone (Merck, p.a.), toluene (Merck, p.a.), and paracetamol (fine powder of pharmaceutical grade, 100.3% on dry basis determined as specified by the European Pharmacopé; Astra Production Chemicals AB) were used without further purification and the water was deionized, distilled, and filtered (0.2 μm). The content of water exerts a strong influence on the solubility of paracetamol in acetone–water mixtures (Granberg and Rasmuson, 2000). The water content in the compounds used is given in Table 1.

Acetone + toluene and acetone + water are miscible at all concentrations, and acetone-rich ternary mixtures also form homogeneous solutions at these temperatures. The mutual miscibility boundary (that is, the curve that divides the single- and the two-phase region) in water + acetone + toluene changes only slightly with temperature between 0 and 30°C (Walton and Jenkins, 1923). The addition of a fourth compound to the water + acetone + toluene system can alter this curve (Hashim et al., 1989). The growth experiments in this study were carried out in the one-phase region and in none of the experiments has a split into two phases been observed.

Apparatus

The experiments are performed in a jacketed 1-L, flat-bottom, glass batch crystallizer with a draft tube and an impeller of the marine propeller type (Figure 1). The filling height of the crystallizer is 150 mm and the diameter is 100 mm. The temperature in the crystallizer, which is controlled by a heating and refrigeration circulator (Julabo MH/FP 35), is kept within ±0.02°C. The Pt-100 resistance thermometer used was calibrated against a mercury precision thermometer (Thermo-Schneider, Wertheim, Germany) having an uncertainty of ±0.01°C.

Procedures

The crystallizer is filled with a solution of water + acetone + toluene (given in Table 2 in mass % for each solvent on a solute-free basis), which is saturated at 3–10 °C above 16°C, depending on the mixture (see also Figure 3). An initial supersaturation (Δc_0) is obtained by cooling at approximately 1°C/min at 100 rpm to 16°C. When the desired temperature is attained (16°C), a known amount (W_0) of sieved seed crystals, of size L_0, are added to this solution and the impeller speed is set to 500 rpm. Small samples of solution are withdrawn periodically, filtered (0.2 μm), and evaporated to dryness, for concentration determination. At the end of the experiment the suspension in the crystallizer is filtered and the product crystals are dried for microscopic inspection and sieve analysis.

The seed crystals were produced by cooling crystallization in water, given that PA has a tendency to form agglomerates when crystallized in water + acetone + toluene mixtures. Saturated solutions of PA in water at 50°C were cooled to 16°C. The cooling rate was 0.5°C/min and the stirring rate was 350 rpm. Small, round crystals were produced. The crystals were filtered, dried, and sieved. A sieve fraction (355–400 μm, DIN 4188) of these crystals was allowed to reshape by growth at 16°C in desupersaturation experiments. This "reshaping" is performed in a solution having the same solvent composition as that in the subsequent growth rate experiment. The crystals were allowed to grow to a size of nearly 500–600 μm, after which they were filtered, dried, sieved, and used as seeds in the growth experiments. In most experiments seeds were from the sieve fraction 500-560 μm. However, in some cases other sieve fractions were used having a mean size from 425 to 595 μm. Photomicrographs of paracetamol crystals obtained from cooling crystallizations are shown in Figure 2a, and an example of

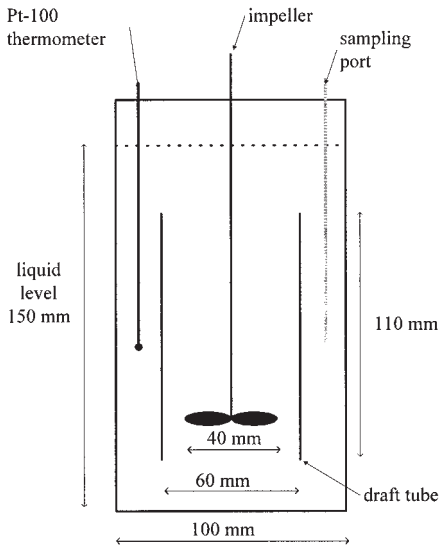

Figure 1. The crystallizer used in the growth experiments.

Table 2. Results of Growth Experiments: Fitted BCF Parameter, A_{BCF}, with 95% Confidence Limits (c.l.), Volume Shape Factor k_V for the Product Crystals, and the Estimated Jackson α-Factor

Water (mass %)	Acetone (mass %)	Toluene (mass %)	A_{BCF} (10^6 m/s)	c.l.* (10^6 m/s)	k_V	α
100	0	0	5.55	1.89	0.61	3.12
93	7	0	6.51	0.57	0.64	2.90
85	15	0	7.69	0.51	0.71	2.68
70	30	0	9.22	0.58	0.54	2.37
50	50	0	9.37	0.20	0.61	2.17
30	70	0	8.31	0.57	0.69	2.03
15	85	0	8.70	0.42	0.75	2.01
7	93	0	8.17	0.71	0.81	2.16
3	97	0	6.48$^{(m2)}$**	0.36	0.70	2.41
0	100	0	6.41	0.59	0.82	2.88
0	95	5	6.66	0.65	0.86	2.92
0	85	15	6.41$^{(m2)}$**	0.31	0.78	3.00
0	70	30	6.16	0.86	0.88	3.21
0	50	50	6.11	1.11	0.64	3.62
3	92.15	4.85	7.59$^{(m8)}$**	0.54	0.77	2.43
3	82.45	14.55	7.33$^{(m2)}$**	0.52	0.73	2.47
3	67.9	29.1	8.90	0.77	0.81	2.57
7	88.35	4.65	9.48	0.68	0.70	2.17
7	79.05	13.95	11.10	1.71	0.73	2.20
7	65.1	27.9	8.91	0.66	0.70	2.27
15	80.75	4.25	10.23	1.55	0.65	2.02
15	72.25	12.75	10.21	1.20	0.66	2.04
30	66.5	3.5	9.30$^{(m2)}$**	0.79	0.71	2.04

*Assuming linear parameter response to the deviations, the 95% confidence limits are estimated from the approximate Hessian at the optimum (Fletcher, 1987).
**Mean value of 2 (m2) or 8 (m8) experiments.

seed crystals and of product crystals, from the (3 + 92.15 + 4.85), are shown in Figures 2b and 2c, respectively.

Eight experiments were performed, on the ternary (3 + 92.15 + 4.85) mixture, using the procedure described above. Conditions that are not expected to influence the growth rate and the growth kinetics, such as initial supersaturation, the size of the seeds, the mass of seeds, and the mass of solvent, were varied, whereas the impeller speed was kept at 500 rpm. At equal driving force ($S = 1.1$), the growth rate becomes on average: 5.4×10^{-8} m s^{-1}, with a standard deviation of 0.4×10^{-8} m s^{-1} for the eight experiments. No systematic influence of these variables has been observed and this standard deviation is regarded as a measure of the reproducibility.

Parameter estimation

The microscopic inspection and the sieve analysis showed that nucleation, breakage, and agglomeration are negligible. The supersaturation in the growth experiments is consumed only by the crystal growth of seeds. If the crystal shape remains unchanged, and growth rate dispersion is negligible, the parameters of a growth rate equation can be estimated by fitting the mass balance equation

$$\Delta c(t) = \Delta c_0 - \left[\left(\frac{L}{L_0}\right)^3 - 1\right]\frac{W_0}{M} \tag{14}$$

directly to the experimental solute concentration measurements (Qiu and Rasmuson, 1990). The crystal size L at time t is calculated by numerical integration of

$$L = L_0 + \int_0^t G(\Delta c)dt \tag{15}$$

where M is the mass of solvent and G (m s^{-1}) is the overall linear growth rate:

$$G = \frac{dL}{dt} \tag{16}$$

The objective function F is the sum-of-squares difference in supersaturation between measurements and predictions:

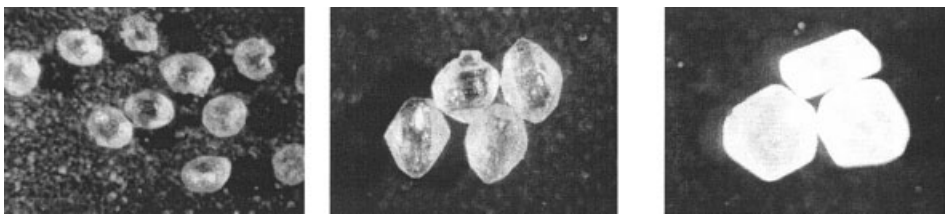

Figure 2. Paracetamol crystals (a) from aqueous solution with a cooling rate of 0.5°C/min, (b) seed crystals, and (c) product crystals from the (3 + 92.15 + 4.85) mixture.

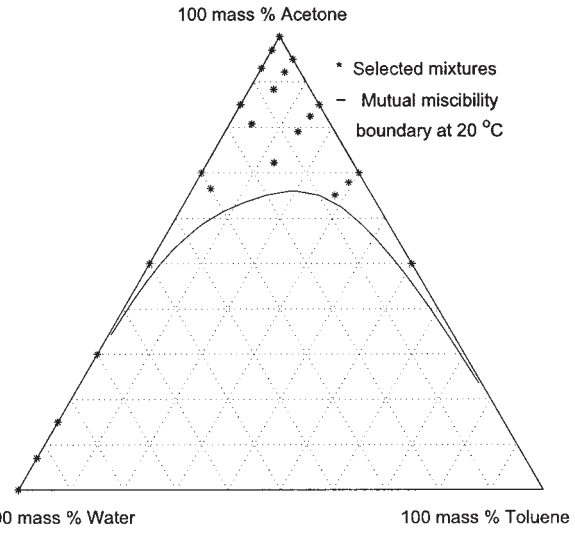

Figure 3. Selected mixtures of water + acetone + toluene and the curve that divides the single- and two-phase regions: redrawn from Walton and Jenkins (1923).

$$F = \sum (\Delta c_{\text{exp}} - \Delta c_{\text{calc}})^2 \quad (17)$$

In the correlation of each experiment an equation for the growth rate dependency on the supersaturation is inserted. Equations 1a, 2, and 3a have been evaluated as well as the overall power-law equation:

$$G = k_g(c - c^*)^g = k_g \Delta c^g \quad (18)$$

Although the power-law equation (Eq. 18) usually gives the best fit to the experimental desupersaturation curve, the B+S (Eq. 3a), and the BCF (Eqs. 1a and 2) models can also describe the experimental measurements very well. Figure 4a shows supersaturation measurements for the (3 + 92.15 + 4.85) mixture and the desupersaturation curves (using Eqs. 18, 1a, 2, and 3) that correspond to the results of the optimization. All these models predict the actual concentration measurements to within 0.3% (which is about the uncertainty of the concentration/solubility measurement). The objective function is shown in Figure 4b.

The driving force

A change in solvent composition automatically changes the driving force for crystallization, given that the solubility is altered. However, in the present work the ambition is to give separate account to driving force effects, to distinguish the influence of the solvent composition as such on the crystal growth rate. Thus, growth rates are to be compared at equal true driving force, that is, equal difference in chemical potential $\Delta\mu$ between the solute in the solution μ^{solution} and in the solid phase μ^{solid}. Assume that the solid crystalline phase is pure and use the pure supercooled melt as reference state (compare Raoult's law). Then, in the saturated solution the activity of the solid and of the solute in the solution are equal, $a^{\text{solid}} = a_{eq} = \gamma_{eq}x_{eq}$, and we may write

$$\frac{\Delta\mu}{kT} = \frac{\mu^{\text{solution}} - \mu^{\text{solid}}}{kT} = \ln\frac{a}{a_{eq}} = \ln\frac{\gamma x}{\gamma_{eq}x_{eq}} = \ln S \quad (19)$$

In the present study, the activity coefficient ratio is estimated by the UNIFAC group-contribution method (Fredenslund et al., 1975). These activity coefficients are based on a Raoult's law approach and on mole fractions. The functional groups in a paracetamol molecule are four aromatic hydrocarbons (Ar–CH), one aromatic carbon with an alcohol group (Ar–COH), one aromatic carbon with an amine group attached (Ar–CNH), and one methyl-carbonyl group (CH_3CO). The group interaction parameters used are those of Hansen et al. (1991). Unfortunately, data for the functional group Ar–CNH are not available. As a first approximation we have chosen to use the group interaction parameters for the Ar–CNH_2 group instead.

Figure 5 shows the calculated activity coefficient ratio from the UNIFAC simulations at 16°C for the binary mixtures. In Figure 5b, x/x_{eq} is kept constant at 1.05. It may be concluded that the influence of nonideality in general is stronger in mixtures with a higher solubility. It has been shown that the trends in the influence of solvent composition and temperature on

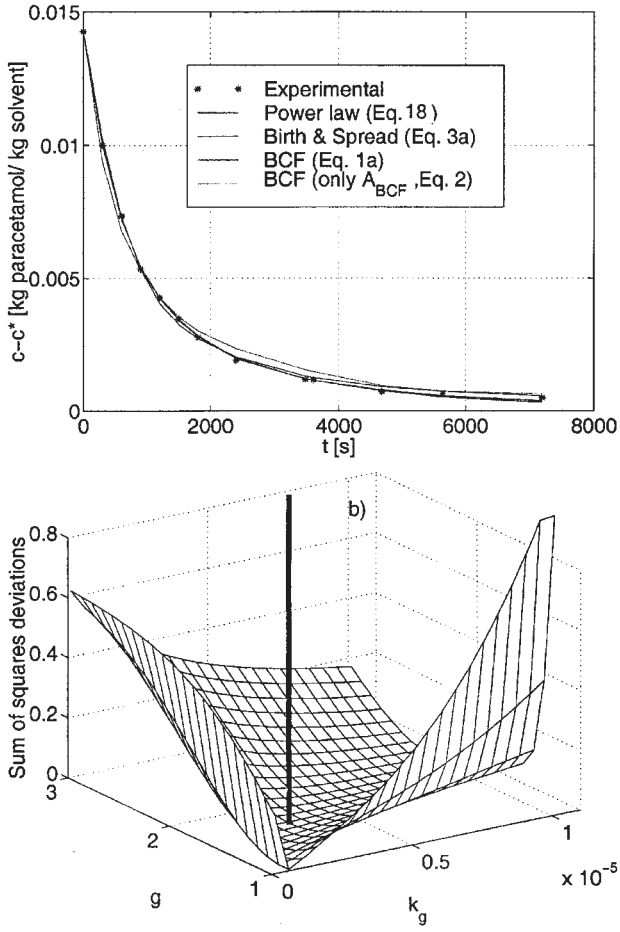

Figure 4. (a) Measured supersaturation vs. time data and calculated desupersaturation curve obtained from the optimizations. (b) Objective function when correlating the power law, Eq. 18.

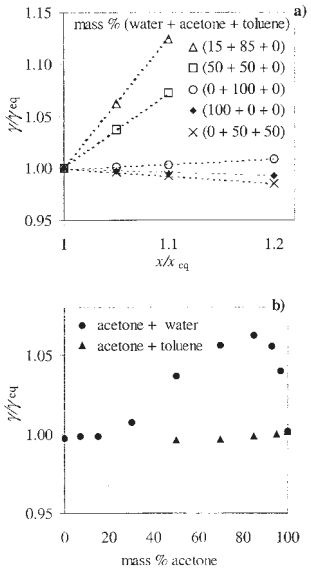

Figure 5. Activity coefficient ratios from the UNIFAC simulations at 16 °C vs. (a) x/x_{eq}, and (b) solvent composition at x/x_{eq} = 1.05.

solubility of PA can be predicted by the UNIFAC approach, although differences in values remain (Gracin et al., 2002; Granberg et al., 2000; Krtalic, 1998). As a first approximation these differences are assumed to cancel out in the predicted activity coefficient ratios.

Results

The influence of the solvent composition on the growth kinetics of paracetamol has been investigated in 23 different water + acetone + toluene mixtures, shown in Figure 3 and Table 2, given in mass % for each solvent on a solute-free basis. These constituted, in addition to pure water and pure acetone, eight binary acetone + water, four binary acetone + toluene, and nine ternary acetone + toluene + water mixtures. The solubility of paracetamol in these solvent mixtures between −5 and +30°C has been reported previously (Granberg and Rasmuson, 2000). The mole fraction solubility of paracetamol in the different mixtures ranges from 0.001 (in water) up to 0.1 [in the (30 + 70 + 0) mixture], which is equivalent to 11 and 400 g paracetamol/kg solvent, respectively.

Overall growth rates

The best fit to experimental desupersaturation curves is usually obtained by the power-law Eq. 18. Thus, this equation is used to initially establish and analyze the influence of the solvent composition.

Figure 6a shows that γ, in the supersaturation range studied, the growth rates (using Eq. 18 with the estimated parameters k_g and g) range from 10^{-9} to 10^{-7} m/s. The lowest growth rate was found in the (0 + 50 + 50) mixture and the highest in the (70 + 30 + 0) mixture. Little is reported on growth rates of paracetamol in different solvents. However, as can be seen in Figure 6b, the overall growth rate in the present work is to a certain extent in agreement with reported face growth rates of paracetamol in water solutions (Finnie et al. 1996; Shekunov et al., 1996).

The influence of solvent composition on the crystal growth rates at equal driving force (S = 1.1) is shown in Figure 7. In binary mixtures, the crystal growth rate exhibits a clear maximum in the water + acetone mixtures, whereas the growth rate decreases monotonously with increasing toluene concentration (Figure 7a) in acetone + toluene mixtures. Water exerts a strong influence on the growth rates in ternary mixtures, as shown in Figure 7b.

The binary results exhibit similarities with the influence of the solvent composition on the solubility (Granberg and Rasmuson, 2000), although the obtained growth rate maximum in the water + acetone mixture is not as pronounced as the corresponding solubility maximum and it occurs at about 40 mass % acetone. Early (Davey, 1982), it was suggested that the growth rate should increase with increasing solubility. The correlation between crystal growth rates of paracetamol in all water + acetone + toluene mixtures and the corresponding solubility mole fraction is shown in Figure 8a. At equal driving force (S = 1.1), there is a weak trend of increasing growth rate with increasing solubility in these mixtures. However, because the solubility spans about two orders of magnitude, the influence is not very clear and strong. In Figure 8b the growth rates at equal c/c^* = 1.05 are plotted vs. the solubility and in this case the influence is more pronounced. If the results are compared at an equal concentration ratio, c/c^* = 1.05, the influence of the solvent composition appears to be stronger. The growth rate range is more than doubled, and the growth rate maximum in the water + acetone mixture is now more pronounced and occurs at about 20 mass % water, which more closely resembles the solubility curve. Thus, by taking into account the nonideality effects in the driving force, the variation in the

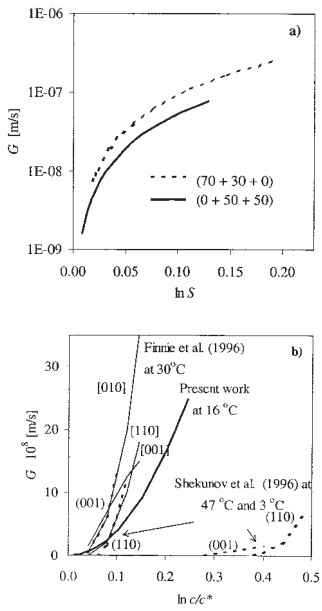

Figure 6. Crystal growth rate of paracetamol vs. supersaturation.

(a) The range of data in the present work. (b) In aqueous solutions at 16°C (present work), and at 3, 30, and 47°C: redrawn from Shekunov et al. (1996) and Finnie et al. (1996).

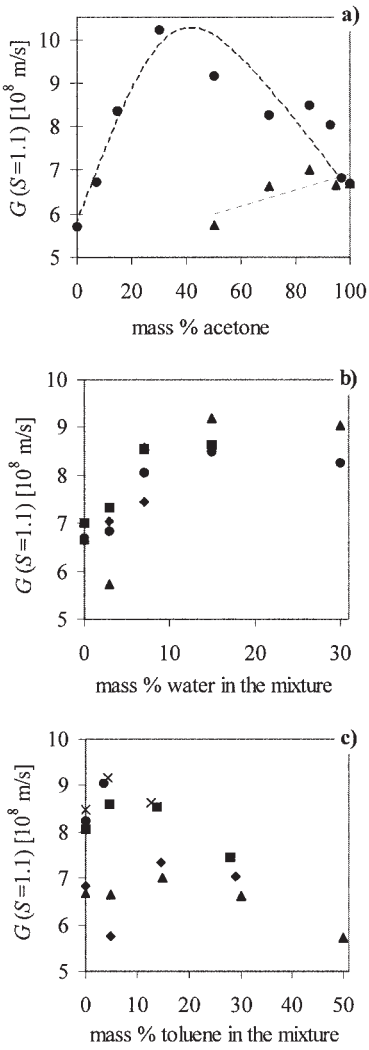

Figure 7. Crystal growth rate of paracetamol vs. solvent composition at equal driving force.

(a) In binary (●) acetone + water and (▲) acetone + toluene mixtures; (b) in ternary mixtures with an acetone/toluene ratio of ●, 100/0; ▲, 95/5; ■, 85/15, and ◆, 70/30; and (c) in ternary mixtures with ●, 30; ×, 15; ■, 7; ◆, 3; and ▲, 0 mass % water.

growth rate with solvent composition is reduced from a factor 5 down to a factor 2.

Evaluation by the BCF theory

In correlating the BCF theory with the experimental desupersaturation curves, it turns out that only a slight decrease in the quality of fit occurs if Eq. 1 is replaced by Eq. 2, as is further examined in the discussion. Correlation of the two-parameter growth rate equations to the experimental data reveals a significant bias between the two parameters because the objective function is shaped like a valley, as shown in Figure 4b. Thus, the confidence in the particular value of each parameter is reduced. For these reasons we apply the parabolic law (that is, Eq. 2) in the following.

The estimated BCF parameter A_{BCF}, obtained by correlation of Eq. 2 to experimental desupersaturation curves, and the corresponding 95% confidence interval are given in Table 2. The influence of solvent composition on A_{BCF} is shown in Figure 9, where the bars illustrate the approximate 95% confidence limits. As can be seen A_{BCF} varies with solvent composition in a manner similar to $G(S = 1.1)$ in Figure 7, which means that the estimated A_{BCF} values satisfactorily capture the effect of solvent composition on the crystal growth rates. According to Eq. 1b, A_{BCF} is inversely proportional to the interfacial energy. As a first approximation we assume that the group $(D_{\mathrm{S}}C_{\mathrm{SE}}\beta\gamma_o/x_{\mathrm{S}})$ is uninfluenced by the solvent composition. Thus the solid–liquid interfacial energy has to account for the full effect of the solvent composition and it is convenient to calculate an interfacial energy ratio as being equal to the inverse of the corresponding ratio of the A_{BCF} values. The value in pure acetone is used as the reference. Results for the binary mixtures are given in Figure 10.

Correlation to enthalpy of dissolution

According to Eq. 4, the interfacial energy is directly proportional to the enthalpy of dissolution:

$$\frac{\gamma_{sl}}{\gamma_{sl,\mathrm{ref}}} \propto \frac{\Delta H^{\mathrm{diss}}}{\Delta H^{\mathrm{diss}}_{\mathrm{ref}}} \tag{20}$$

where "ref" again refers to pure acetone. Thus, the growth rate should be inversily proportional to the enthalpy of dissolution. The solid and the dotted lines in Figure 10a illustrate enthalpy of dissolution ratio as estimated by Eqs. 12 and 13. Solubility values reported by Granberg and Rasmuson (2000) are used. The enthalpy of fusion ΔH^{f}_{m} (27.1 kJ mol^{-1}) at the melting point T_m (443.6 K) was determined by differential scanning calorimetry (Granberg and Rasmuson, 1999).

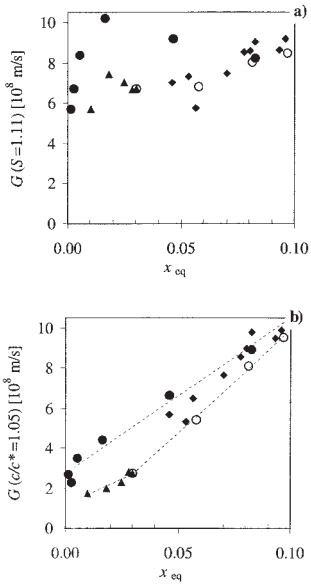

Figure 8. Crystal growth rate of paracetamol vs. solubility, (a) at S = 1.1; (b) at c/c^* = 1.05, in ●, acetone + water (15–100% water); ○, acetone + water (0–15% water); ▲, acetone + toluene; and ◆, water + acetone + toluene.

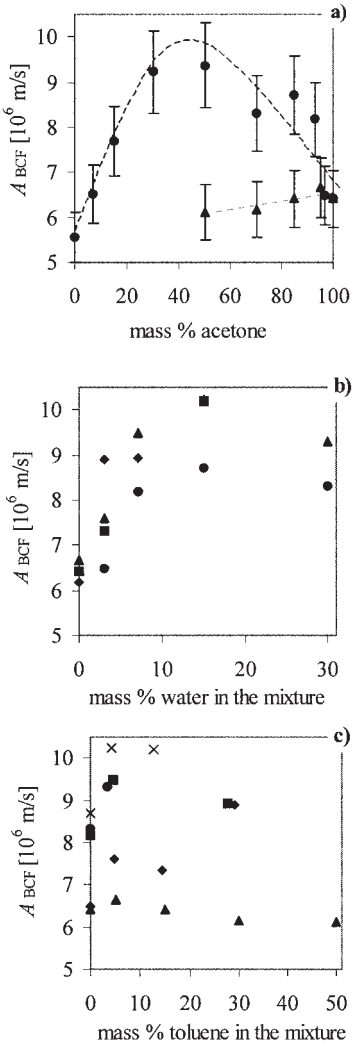

Figure 9. Influence of solvent composition on A_{BCF}.

(a) In binary (●) acetone–water and (▲) acetone–toluene mixtures; (b) in ternary mixtures with an acetone/toluene ratio of ●, 100/0; ▲, 95/5; ■, 85/15, and ◆, 70/30; and (c) in ternary mixtures with ●, 30; ×, 15; ■, 7; ◆, 3; and ▲, 0 mass % water.

The contribution from the heat capacity term in Eq. 12 is often neglected (Klug, 1993; Walas, 1985), that is, $\Delta C_p = 0$ (Figure 10a). However, it has been reported that this can lead to significant errors (Grant and Higuchi, 1990; Neau et al. 1997; Snow et al., 1986). Hildebrand et al. (1970) suggested that ΔC_p could be approximated with the entropy of fusion at the melting point ($\Delta S_m^f = \Delta H_m^f / T_m \approx \Delta C_p$), which becomes 61.1 J mol^{-1} K^{-1} for PA using our own data. A better approximation is probably to take the heat capacity difference at the melting point. It is possible to measure the heat capacity for the melt above the melting point, and for the solid below the melting point by using DSC. The results can be extrapolated to the melting point, as illustrated by Figure 11. For paracetamol this value becomes ΔC_p = 99.8 J mol^{-1} K^{-1} (Neau et al., 1997).

However, the heat capacity term in Eq. 12 actually involves an integration of the heat capacity difference from T to the melting point. As is suggested in Figure 11, the heat capacity

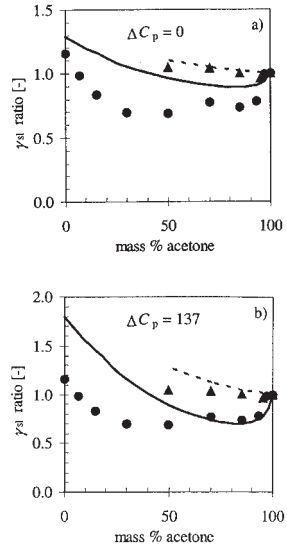

Figure 10. Experimental (●, acetone + water; ▲, acetone + toluene), and predicted [acetone + water (solid line); acetone + toluene (dotted line)] γ_{sl} ratio, with different heat capacity difference: (a) $\Delta C_p = 0$; (b) $\Delta C_p = 137$ J/mol K.

curves for the solid and the melt, respectively, may have different slopes, and thus the heat capacity difference is not constant over the temperature range of integration. Unfortunately, the heat capacity of the melt refers to a hypothetical supercooled liquid and cannot be directly measured. Thus, it seems reasonable to extrapolate the curve for the melt into the supercooled region and actually carry out the integration in Eq. 12, over a heat capacity difference that varies with temperature. In that case the temperature-weighted mean value of the heat capacity difference becomes about 137 J mol^{-1} K^{-1}, over the temperature range [289°C, 443.6°C]. If this value is introduced into Eq. 12 we obtain the result shown in Figure 10b. Using

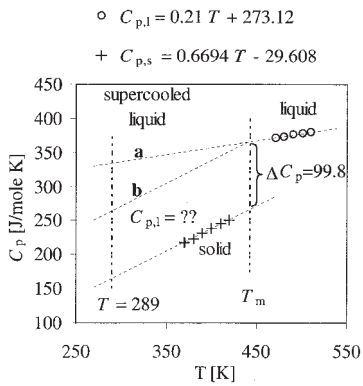

Figure 11. Heat capacities of solid and molten paracetamol determined by differential scanning calorimetry. [Redrawn from Neau et al., 1997.]

Different dotted lines show the assumed heat capacity behavior for the supercooled melt. Constant ΔC_p is route **b**. Route **a** is reached by extrapolating $C_{p,l}$ from above the melting point temperature down to the temperature of the solution.

ΔC_p values of 61.1 or 99.8 J mol^{-1} K^{-1} leads to results between those of Figure 10a and Figure 10b.

As can be seen in Figure 10, although there is qualitative resemblance between the estimated ratios (lines) and the experimental data (points), the minimum in acetone + water mixtures cannot be fully captured. The enthalpy of dissolution in Eq. 12 receives contributions from three terms. The entropy of fusion term is $\Delta S_m^f/R = 7.4$, and the heat capacity difference term $\Delta C_p \ln(T_m/T)/R$ becomes 0, −3.1, −5.1, and −7.0 for ΔC_p = 0, 61.1, 99.8, and 137 J mol^{-1} K^{-1}, respectively, and they depend only on pure component properties. The contribution of the solvent-dependent term expressing the entropy of mixing of an ideal mixture, $-\ln x_{eq}(T)$, is between 2.5 and 6.6, depending on the mixture. As shown previously (Granberg and Rasmuson, 2000) the system paracetamol dissolved in water + acetone + toluene mixtures is highly nonideal with both negative and positive deviations from Raoult's law, depending on the solvent composition. The regular solution theory is known to fail for systems where the solvent and the solute are polar, when hydrogen bonding leads to specific molecular orientation effects and when the solvent and the solute are rather different in size (Grant and Higuchi, 1990). Thus, we need to consider a more adequate representation of the entropy of mixing.

In UNIFAC the activity coefficient of the solute in the saturated solution, defined on the basis of Raoult's law, is given by (Prausnitz et al., 1999, p. 219; Walas, 1985, p. 119):

$$\ln \gamma = \ln \gamma^{\mathrm{R}} + \ln \gamma^{\mathrm{C}} = \frac{G^E}{RT} = \frac{H^E - TS^E}{RT} \tag{21}$$

where the residual part (R) reflects the excess enthalpy of mixing resulting from interaction energies and the combinatorial part (C) reflects the excess entropy of mixing stemming from differences in size and shape (Prausnitz et al., 1999). Thermodynamic quantities are the partial molar quantities and the upper index E stands for "excess," denoting the difference between the value for the real solution and that of a corresponding ideal solution. Thus, we adopt

$$S^E \approx -R \ln \gamma^{\mathrm{C}} \tag{22}$$

and the partial molar entropy of mixing is obtained by adding the excess entropy to the ideal entropy of mixing:

$$\Delta S^{\mathrm{mix}} = \Delta S^{\mathrm{ideal}} + S^{\mathrm{E}} = -R \ln x_{eq} - R \ln \gamma^{\mathrm{C}} = -R \ln x_{eq}\gamma^{\mathrm{C}} \tag{23}$$

The entropy of mixing is calculated using the interaction parameters of Hansen et al. (1991). If Eq. 23 is used to replace Eq. 11, and the integrated heat capacity difference value (ΔC_p = 137 J/mol K) is used we obtain the result shown in Figure 12. In particular, the data in the binary acetone–water solution are described quite well and Figure 12b shows that in fact the data in ternary mixtures are also quite nicely predicted. The corresponding calculated entropies of mixing are given in Table 3. Quite negative excess entropies of mixing are predicted for the acetone–water solutions rich in water, which describe that when paracetamol is dissolved in the solvent, the resulting solution becomes more ordered than the corresponding ideal mixture. In fact, the excess entropy of mixing for the acetone + water mixtures itself is large and negative (Blandamer and Burgess, 1975). The introduction of acetone into water leads to a reduction of the degrees of freedom of the neighboring water molecules (Franks, 1983). We have also evaluated two other classical equations to estimate nonideal entropies of mixing: the Flory–Huggins equation (Hildebrand et al., 1970) and the more recent equation proposed by Huyskens and Haulait-Pirson (1985). Both equations fail to predict large negative values for the excess entropy of mixing, and the ideal entropy of mixing leads to a better description of our data.

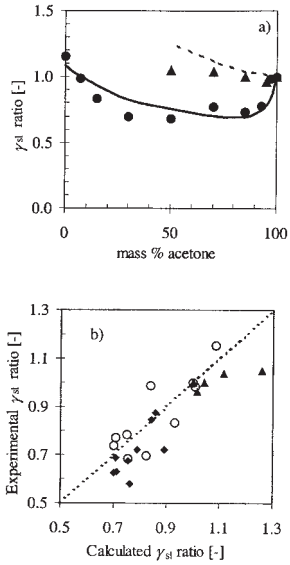

Figure 12. Experimental interfacial energy ratios and predicted using ΔC_p = 137 J/mol K and the UNIFAC entropy of mixing calculated by Eq. 23.

(a) Binary data, experimental (●, acetone + water; ▲, acetone + toluene) and predicted [acetone + water (solid line); acetone + toluene (dotted line)]; (b) binary and ternary data (○, acetone + water; ▲, acetone + toluene; ◆, water + acetone + toluene).

Discussion

Experimental data

By the seeded isothermal desupersaturation method, the overall linear growth rate of the entire crystal is obtained from the rate of supersaturation decay. The shape factor does not explicitly influence the growth rate value obtained, but it is assumed that the shape in each experiment is constant. However, depending on the solvent composition, the seeds may have different shapes and, to make a proper comparison, we need to correct the overall growth rate for this shape difference. An average face growth rate (G_{hkl}^s) can be defined as

$$\frac{dW}{dt} = n_C \rho_C \sum_{hkl} A_{hkl} G_{hkl} = n_C \rho_C A_{\mathrm{tot}} G_{hkl}^s = n_C \rho_C k_A L^2 G_{hkl}^s \tag{24}$$

and it can be shown that

Table 3. Partial Molar Entropy of Mixing of Paracetamol in Different Solvent Mixtures of Water + Acetone + Toluene

Water (mass %)	Acetone (mass %)	Toluene (mass %)	ΔS^{mix}* (J mol^{-1} K^{-1})	S^{E}** (J mol^{-1} K^{-1})	$\Delta S^{mix\,\dagger}$ (J mol^{-1} K^{-1})
100	0	0	55.0	−21.2	33.8
93	7	0	49.5	−18.4	31.1
85	15	0	43.9	−15.1	28.6
70	30	0	34.1	−8.9	25.2
50	50	0	25.5	−2.8	22.8
30	70	0	20.7	0.2	20.9
15	85	0	19.4	1.1	20.5
7	93	0	20.9	1.4	22.3
3	97	0	23.7	1.6	25.3
0	100	0	29.1	1.7	30.8
0	95	5	29.6	1.7	31.3
0	85	15	30.6	1.6	32.3
0	70	30	33.1	1.6	34.8
0	50	50	38.1	1.4	39.6
3	92.15	4.85	23.9	1.1	25.0
3	82.45	14.55	24.4	0.8	25.2
3	67.9	29.1	25.6	0.7	26.3
7	88.35	4.65	21.0	0.5	21.5
7	79.05	13.95	21.3	1.5	22.8
7	65.1	27.9	22.1	1.5	23.6
15	80.75	4.25	19.5	1.5	21.0
15	72.25	12.75	19.7	1.4	21.1
30	66.5	3.5	20.8	1.4	22.1

Note: A volume fraction mean value of the molar volume for the solvent is used in binary and ternary solvent mixtures (that is, when there is more than one solvent).
*Ideal, calculated from Eq. 11.
**Excess (from UNIFAC simulations) calculated from Eq. 22.
†Ideal + Excess, calculated from Eq. 23.

$$G^{s}_{hkl} = \frac{3k_V}{k_A} G \tag{25}$$

Thus to compare the growth rate from different experiments we should correct for differences in shape. In the present work, the crystal size is determined as the arithmetic mean aperture size of the upper and the lower sieves of the particular sieve fraction. Figure 13 shows the size distribution from a sieving analysis of seed crystals and of product crystals. Volumetric shape factors have been determined by counting and weighing 200 crystals from each sieve fraction. The seed crystals (L_0 = 475 μm) are from the sieve fraction 450–500 μm (DIN 4188), and have a shape factor, k_V = 0.64 ($\pm$0.11). The product crystals from all the growth experiments had the same overall crystal shape: rounded hexagons (Figure 2c). The mass-weighted mean value (over all the sieve fractions) of the shape factors are given in Table 2. The value varies from 0.54 to 0.88. There is a slight tendency for k_V to become lower at higher concentrations of toluene or water. Microscope observations suggest that slightly more elongated crystals are formed with increasing toluene concentration and that with increasing water concentrations the crystals become slightly more flat. These observations are supported by single-crystal experiments in which the habit changes from round-shaped crystals to needle-like crystals with increasing toluene concentration, and the crystals from water were flat (Granberg and Rasmuson, 1997). If the area shape factor is approximated by (Matz, 1982) k_A = 2 + 4k_V, 3k_V/k_A ranges from 0.39 to 0.48. If the face growth rate of Eq. 25 is plotted instead of the overall growth rate in Figure 7, the y-axis scale shifts but the overall appearance is unchanged. Thus, the influence of the shape effect is regarded to be small compared to the influence of the solvent composition and of the driving force, and is therefore neglected. Equation 24 also shows that, even though the growth models concern only the growth of individual faces, there is a fairly direct relation to the experimentally determined overall growth rate if the shape is constant throughout each growth experiment.

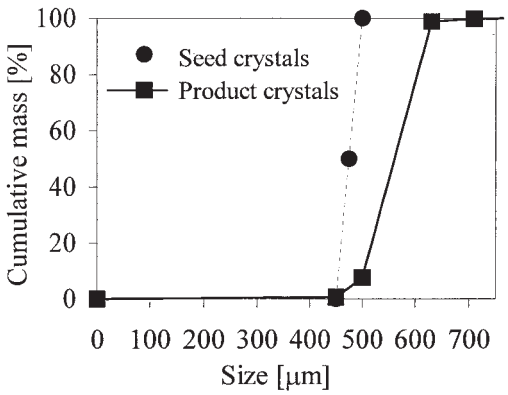

Figure 13. Seed crystal and product crystal size distributions.

Two polymorphic forms of paracetamol are generally mentioned in the literature. A monoclinic form (Haisa et al., 1976; Welton et al., 1988), which is the usual pharmaceutical form, and an orthorhombic form (di Martino et al., 1996; Haisa et al., 1974; Nürnberg et al., 1982; Sohn, 1990). X-ray powder diffraction analysis and differential scanning calorimetry (DSC) of the product crystals in the present work did not indicate any polymorphism.

Growth model

In the evaluation of experimental data we assume the influence of the boundary layer diffusion to be negligible. Experi-

ments have also been carried out at 400 and 800 rpm on the ternary (3 + 92.15 + 4.85) mixture. Figure 14 shows the growth rates at equal driving force ($S = 1.1$), as estimated by the parameters k_g and g, obtained by correlation of the power-law Eq. 18 to the desupersaturation curve of these experiments. There appears to be no influence of the impeller speed on the growth rates. In addition, from previous work, in acetone–toluene mixtures (Granberg and Rasmuson, 1997) and in acetone–water mixtures (Granberg et al., 1999), where the power-law equation was used, values of the growth order g were always >1. These results support the assumption that growth is controlled by the surface integration step.

A simplified version of the BCF model has been adopted (Eq. 2). Figure 15 shows the estimated parameters A_{BCF} and B_{BCF} when Eq. 1a is adopted vs. solvent composition, in binary water + acetone + toluene mixtures. As can be seen the parameter B_{BCF} is almost independent (or no clear influence) of solvent composition in the binary mixtures, with values about 0.06. It has been shown (Bennema et al., 1973) that most measured (G or G_{hkl}) vs. (ln S) curves can be fitted with approximately $10^{-1} \leq B_{\mathrm{BCF}} \leq 10^{-2}$.

The α-factor can be estimated by Eqs. 5 and 6. The anisotropy factor is estimated from CERIUS^2 (1995) simulations. Paracetamol crystallizes in a P21/a monoclinic space group, with the unit cell parameters $a = 12.93$ Å, $b = 9.40$ Å, $c = 7.10$ Å, and $\beta = 115.9$ ° (Haisa et al., 1976). Crystal packer and molecular mechanics was used to minimize the crystal structure and, for the attachment energy method (AE) prediction, the Dreiding2 force field was used. The predicted AE morphologies are in good agreement with morphologies reported by Green and Meenan (1996). The total lattice energy ($E^{\mathrm{latt}} = 110$ kJ mol^{-1}) and the attachment energies E^{att}_{hkl} (between 23 to 39 kJ mol^{-1} depending on the face) are in agreement with attachment energies reported by Shekunov and Grant (1997). The calculated anisotropy factor (using Eq. 6) becomes between 0.6 and 0.8 depending on the face, which is within the range reported by Sloan and McGhie (1988). The enthalpy of dissolution is estimated by Eq. 12, using the integrated value of the heat capacity difference ($\Delta C_p = 137$ J mol^{-1} K^{-1}) and replacing the ideal mixing entropy by Eq. 23. The α-values for $\xi_\alpha = 0.7$ are given in Table 2 and range from 2 to 4. According to this we would expect the B+S mechanism to dominate (Bourne and Davey, 1976; Gilmer and Bennema, 1972). In fact, the B+S model provides a correlation of the experimental desupersaturation data that is almost as good as that of the BCF theory. There is a tendency for the B+S model to fail at low level of supersaturation, but this is in accordance with theory (Myerson and Ginde, 1993). In the B+S model the dependency on the interfacial energy is found in the exponential term where $B_{\mathrm{B+S}}$ is proportional to γ^2_{sl} (Eq. 3c). However, in the parameter estimation, the influence of solvent composition is found primarily in the $A_{\mathrm{B+S}}$ parameter. If the $A_{\mathrm{B+S}}$ value is assumed to be equal for all experiments, the correlation to each experiment becomes a one-parameter determination of the $B_{\mathrm{B+S}}$ parameter. In Figure 15c is shown the estimated parameter $B_{\mathrm{B+S}}$ from Eq. 3 vs. solvent composition, in binary water + acetone + toluene

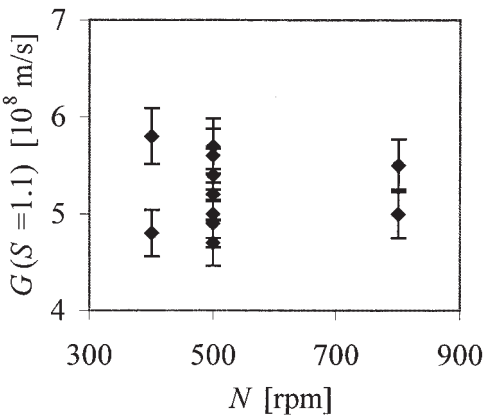

Figure 14. Influence of the hydrodynamic conditions on crystal growth rates at equal driving force.

The uncertainty bars are calculated from the approximate 95% confidence limits of the estimated parameters k_g and g.

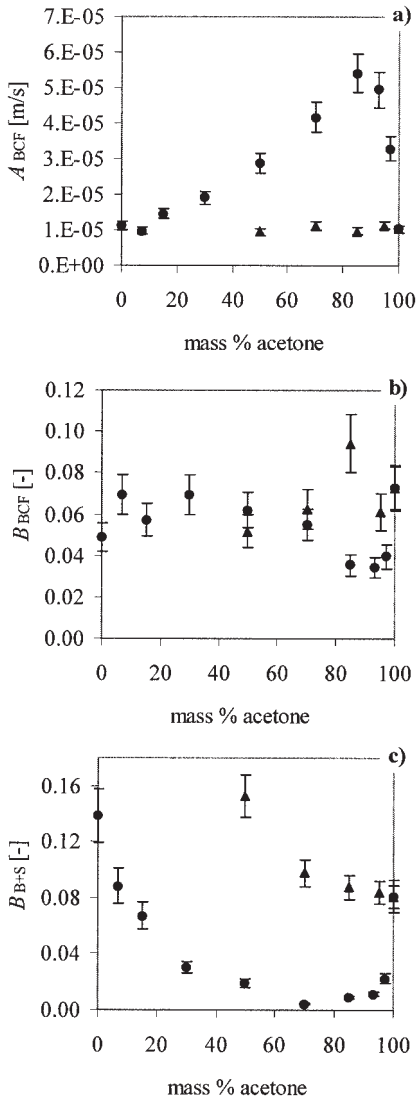

Figure 15. Influence of solvent composition in binary (●) acetone–water and (▲) acetone–toluene mixtures, (a) and (b) on A_{BCF} and B_{BCF} as determined in two-parameter optimizations, and (c) on $B_{\mathrm{B+S}}$ when determined using a value on $A_{\mathrm{B+S}}$ being equal for all experiments.

mixtures. As shown the result is quite close to that obtained by the BCF model, concerning the overall appearance of the relation between the solvent composition and the experimental interfacial energy ratios. However, the solvent composition has a stronger influence.

In summary, for the present data the two-parameter BCF equation behaves more adequately than the two-parameter B/S equation. It is furthermore reported that for paracetamol in aqueous solutions, growth usually proceeds by a dislocation mechanism (Finnie et al., 1996, 1999; Shekunov and Grant, 1997). In addition, the calculated α-value depends substantially on the approximations used: if $\Delta C_p = 0$ is used, α-values between 7 and 8 are obtained. It has also been reported that α-values, based on the equivalent wetting condition, are usually too low (Bennema and van der Eerden, 1987), even though it is claimed to be a useful assumption for a number of organic molecules (Davey et al., 1988; Elwenpoek et al., 1987; Klug, 1993).

Interfacial energy and density of growth sites

Interfacial energy values for paracetamol obtained by induction time measurements in acetone + water mixtures have been reported (Granberg et al., 2000). In a binary mixture with 70% water the value was found to be $\gamma_{sl} = 1.4$ mJ m^{-2}. Using this value and assuming that the group $(D_S C_{SE} \beta \gamma_o / x_S)$ is constant, the interfacial energy calculated from the experimental A_{BCF} values in Table 2 ranges from 1.2 to 2.3 mJ m^{-2}. In water the value becomes 2.3 mJ m^{-2}, which is close to the value of 1.8 mJ/m^2 estimated from cooling crystallization experiments (Hendriksen and Grant, 1995; Prasad et al., 1999). However, interfacial energies calculated by Eq. 4 are clearly higher.

In the BCF model, the distance between neighboring turns of the spiral y_0 and the average distance between neighboring kinks in the step x_0 are given by (Mersmann, 1995; Nielsen, 1984)

$$y_0/a_c = 19\gamma_e/kT \ln S \tag{26}$$

$$x_0/a_c = \exp(\gamma_e/kT)/\sqrt{S} \tag{27}$$

The intermolecular distance a_c is often approximated by $a_c = V_m^{1/3}$ (Nielsen, 1984; Nyvlt et al., 1985; Ohara and Reid, 1973). The edge work γ_e is the interfacial energy of the surface exposed in the step and may be expressed in terms of the interfacial energy as $\gamma_e = a_c^2 \gamma_{sl} = V_m^{2/3} \gamma_{sl}$ (Mersmann, 1995).

In the binary mixtures at $S = 1.1$, x_0 ranges from 6.1 to 6.8 Å and y_0 from 120 and 220 Å, based on the range of interfacial energy values for the different mixtures given above. The principal dependency of x_0 and y_0 on the solvent composition resembles that of the interfacial energy ratio shown in Figure 12. In the acetone–water mixtures both parameters exhibit a minimum at about 40 mass % of acetone. The kink distance x_0 is not very different from the intermolecular distance and the interplanar spacing estimated from CERIUS^2 simulations, and there is little difference in "kink density" between the different mixtures. However, except for regions of low concentration of either solvent, y_0 is clearly lower in acetone + water mixtures than in acetone + toluene mixtures. The growth units need to diffuse a much shorter distance on the terrace before actual integration into the lattice, which leads to higher growth rates.

Activity coefficients and enthalpy of dissolution

The estimation of activity coefficients by UNIFAC simulations have to be regarded as approximate, given that the UNIFAC interaction parameters are derived from vapor–liquid equilibrium data, and because data for the functional group A–CNH are not available. As an approximation, the A–CNH$_2$ group was used instead. The A–CNH$_2$ group is a fair hydrogen-bonding donor and a very good hydrogen-bonding acceptor. However, the A–CNH group in paracetamol is a good hydrogen-bonding donor, whereas it is not a hydrogen-bonding acceptor. The A–CCH$_2$ group could have been used as a substitute instead (Gracin et al., 2002). This group is neither a hydrogen-bond acceptor nor a donor. If this latter group is used as a substitute in the UNIFAC simulations, the influence of solvent composition, at $x/x_{eq} = 1.05$, on the predicted activity coefficient ratios is not as strong as with the A–CNH$_2$ substitute. This leads to a more pronounced influence of solvent composition on the growth rates at $S = 1.1$, and to a less successful prediction of the interfacial energy ratio by estimation of the heats of dissolution because the choice of substituting functional group has very little influence on the combinatorial part of the activity coefficient.

In the estimation of the enthalpy of dissolution, standard thermodynamic data are used like the enthalpy of melting and the melting point temperature, as well as the heat capacity vs. temperature for the melt and the solid. An important weakness is that we need to extrapolate far into the supercooled region and thus the estimated enthalpy of fusion at the temperature of growth can only be approximate. The solution is nonideal and thus the entropy of mixing involves the estimation of excess entropy and again this involves the uncertainties described above for the UNIFAC approach, even though this estimation is regarded to be more safe in that it involves the estimation of only the combinatorial part and thus only volume and area of functional groups.

The enthalpy of dissolution in the nearly saturated solution as estimated by Eqs. 12 and 23 using $\Delta C_p = 137$ J mol^{-1} K^{-1} ranges from 7 to 12 kJ/mol. For organic substances dissolved in organic solvents, the enthalpy of dissolution at infinite dilution is usually between 5 and 20 kJ/mol (Mullin, 1993). Because the dilution enthalpy often is small compared to the dissolution enthalpy (Mullin, 1993), these values approximately hold also for the enthalpy of dissolution in a nearly saturated solution. Often an approximate enthalpy of dissolution (Mullin, 1993; van Hoof et al., 1998) is estimated from solubility data by plotting ln x_{eq} vs. $1/T$ in a van't Hoff plot. By using our previously reported solubility data (Granberg and Rasmuson, 2000) we obtain van't Hoff enthalpies of dissolution ranging from 10 to 25 kJ/mol for the present mixtures. These values are much higher than those calculated by Eq. 12 combined with Eq. 23, especially in acetone + water mixtures containing 10 to 50 mass % acetone, and they do not correlate well with growth rate results.

Conclusions

The crystal growth rates of paracetamol have been determined in binary and ternary water + acetone + toluene mix-

tures by seeded isothermal desupersaturation experiments at 16°C. At equal logarithmic supersaturation ratio ln(c/c^*) the growth rate depends significantly on the solvent composition. Compared at equal thermodynamic driving force ($\Delta\mu$) the influence is significantly weaker, but there is still a variation of about a factor 2, suggesting that there is an influence arising from chemical interactions of the solvent. In acetone + toluene mixtures, increasing toluene concentration leads to decreasing growth rates. In acetone + water mixtures, the growth rate of paracetamol crystals increases to a maximum at approximately 40 mass % water before it decreases in a similar manner as does the solubility of paracetamol in these mixtures. A surface diffusion spiral growth (BCF) model gives a good description of the experimental desupersaturation data. The influence of the solvent composition at equal driving force can be described in terms of the interfacial energy between the solid and the solution. It is shown that a reasonable prediction of the influence of the solvent composition on the interfacial energy is obtained if a proper estimation of the enthalpy of dissolution can be obtained. For the case of paracetamol crystals growing in water + acetone + toluene mixtures this estimation needs to include an estimation of the entropy of fusion at the temperature of growth and an estimation of the nonideal entropy of mixing.

Acknowledgments

The authors gratefully acknowledge the activity coefficient calculations of MSc Sandra Gracin; the financial support of The Industrial Association for Crystallization Research and Technology (IKF) and The Swedish National Board for Industrial and Technical Development (NUTEK); Astra Production Chemicals for providing the paracetamol; and Dr. Marco Mattos (Universität Bremen) for assisting in the (CERIUS) molecular modeling.

Notation

A_{BCF} = BCF parameter, m s^{-1}
A_{B+S} = B+S parameter, m s^{-1}
A_{hkl} = area of a face, m^2
A_i = area of crystal face i, m^2
A_{tot} = $\sum_{hkl} A_{hkl}$ = area of a crystal, m^2
a = activity in supersaturated solution
a_c = intermolecular distance, m
a_{eq} = activity of solute in saturated solution
a^{solid} = activity of solute in solid phase
$a^{solution}$ = activity of solute in solution
B_{BCF} = BCF parameter
B_{B+S} = B+S parameter
C_{SE} = equilibrium surface concentration of the solute on the surface if $\sigma = 1$
$C_{p,l}$ = heat capacity of the melt, J mol^{-1} K^{-1}
$C_{p,s}$ = heat capacity of the solid, J mol^{-1} K^{-1}
ΔC_p = difference in heat capacity between the supercooled melt and the pure solid, Eq. 13, J mol^{-1} K^{-1}
c = concentration, kg/kg solvent
c^* = solubility, kg/kg solvent
Δc = concentration driving force, supersaturation, $c - c^*$, kg/kg solvent, lower index: "exp" means experimental value, "calc" means calculated
Δc_0 = initial concentration driving force, kg/kg solvent
D_S = solute diffusion coefficient on the surface, m^2 s^{-1}
E^{latt} = total lattice energy, J mol−1
E^{att}_{hkl} = attachment energy, J mol^{-1}
F = value of the objective function in parameter determination
G = overall linear crystal growth rate, m s^{-1}
G^E = excess Gibbs free energy, J mol^{-1}
G_{hkl} = face growth rate, m s^{-1}
G^s_{hkl} = overall face growth rate defined in Eq. 24, m s^{-1}
g = growth order with respect to supersaturation
H^E = excess enthalpy, J mol^{-1}
ΔH^{diss} = enthalpy of dissolution, $-\Delta H^{cryst}$, J mol^{-1}
ΔH^f_m = enthalpy of fusion at the melting point, J mol^{-1}
h = step height or lattice spacing, m
k = Boltzmann constant, R/N_A, 1.38 × 10^{-23} J K^{-1}
k_g = rate constant in power law growth rate equation, m s^{-1}
k_A = A_{tot}/L^2 = area shape factor
k_V = volume shape factor
L = characteristic size of crystal, m
L_0 = size of seed crystal, m
M = mass of solvent, kg
M_C = mass of a crystal, kg
M_v = molecular weight, paracetamol, 0.15117 kg mol^{-1}
N = impeller rotation speed, rpm
N_A = Avogadro's number, 6.023 × 10^{23} mol^{-1}
n_C = number of crystals per kg solvent, nos. kg^{-1}
n_1 = equilibrium number of monomers on the surface per unit area, nos. m^{-2}
r^* = critical radius of a 2D nucleus, m
R = gas constant, 8.314 J mol^{-1} K^{-1}
S = supersaturation ratio, a/a_{eq}
S^E = excess entropy, J mol $^{-1}$K^{-1}
ΔS^{diss} = entropy of dissolution, J mol−1 K^{-1}
ΔS^f = entropy of fusion, J mol^{-1} K^{-1}
ΔS^f_m = entropy of fusion at the melting point, J mol^{-1} K^{-1}
ΔS^{ideal} = entropy of mixing of ideal solution, J mol−1 K^{-1}
ΔS^{mix} = entropy of mixing, J mol−1 K^{-1}
T = temperature, K
T_m = melting point, K
t = time, s
V_m = volume of a molecule, $M_v/\rho_c N_A$, paracetamol, 1.942 × 10^{-28} m^3
$\bar{v}$ = mean rate of adsorption of molecules on the surface
W = mass of crystals per kg solvent, kg/kg
W_0 = mass of seeds per kg solvent, kg/kg
x = concentration, mole fraction
x_{eq} = solubility, mole fraction
x_S = mean diffusion distance on the surface, m
x_0 = average distance between neighboring kinks, m
y_0 = average distance between neighboring turns (step length) in spiral growth, m

Greek letters

α = surface roughness/alpha factor
β = retardation factor for a linear step
γ = activity coefficient
γ^C = activity coefficient, combinatorial
γ^R = activity coefficient, residual
γ^x/γ_{eq} = activity coefficient ratio, mole fraction based, supersaturated/saturated
γ_e = edge free energy, J
γ_{sl} = interfacial energy between solid and liquid, J m^{-2}
γ_o = retardation factor for a kink
μ = chemical potential, J mol^{-1}
$\Delta\mu$ = chemical potential driving force, J mol^{-1}
μ_{eq} = chemical potential of solute in saturated solution, J mol^{-1}
μ^{solid} = chemical potential of solute in solid phase, J mol^{-1}
$\mu^{solution}$ = chemical potential of solute in solution, J mol^{-1}
$\rho = \rho_c$ = density, paracetamol, 1293 kg m^{-3}
ξ_α = surface anisotropy factor
ξ_γ = fraction of enthalpy of dissolution corresponding to unsatisfied bonding

Literature Cited

Ålander, E. M., and Å. C. Rasmuson, "Characterization of Paracetamol Agglomerates by Image Analysis and Strength Measurement," *Powder Technol.*, **130**, 298 (2003).
Ålander, E. M., M. Uusi-Penttilä, and Å. C. Rasmuson, "Agglomeration of

Paracetamol during Crystallization in Pure and Mixed Solvents," *Ind. Eng. Chem. Res.*, **43**(2), 629 (2004).
Bennema, P., "Growth and Morphology of Crystals, " *Handbook of Crystal Growth*, D. T. J. Hurle, ed., Elsevier Science, Amsterdam, Vol. 1a (1993).
Bennema, P., J. Boon, C. van Leeuwen, and G. H. Gilmer, "Confrontation of the BCF Theory and Computer Simulation Experiments with Measured (R, σ) Curves, " *Kristall. Technik*, **8**(6), 659 (1973).
Bennema, P., and G. H. Gilmer, "Kinetics of Crystal Growth, " *Crystal Growth: An Introduction*, P. Hartman, ed., North-Holland, Amsterdam, pp. 263–327 (1973).
Bennema, P., and O. Söhnel, "Interfacial Surface Tension for Crystallization and Precipitation from Aqueous Solutions, " *J. Cryst. Growth*, **102**, 547 (1990).
Bennema, P., and J. P. van der Eerden, "Crystal Graphs, Connected Nets, Roughening Transition and the Morphology of Crystals, " *Morphology of Crystals*, I. Suangawa, ed., Terra Scientific, Tokyo, Japan, p. A1 (1987).
Blandamer, M. J., and J. Burgess, "Kinetic Reactions in Aqueous Mixtures," *Chem. Soc. Rev.*, **4**, 55 (1975).
Bourne, J. R., and R. J. Davey, "The Growth of Hexamethylene Tetramine Crystals from Ethanolic Solutions, " *J. Cryst. Growth*, **34**, 230 (1976).
Bujac, P. D. B., and J. W. Mullin, "A Rapid Method for the Measurement of Crystal Growth Rates in a Fluidized Bed Crystallizer, " *Proceedings of the Symposium on Industrial Crystallization*, Institution of Chemical Engineers, London, p. 121 (1969).
Burton, W. K., N. Cabrera, and F. C. Frank, "The Growth of Crystals and the Equilibrium Structure of Their Surface," *Philos. Trans. R. Soc. Lond. A*, **A243**, 299 (1951).
CERIUS^2, *Molecular Modeling Software for Materials Research*, version 2.0, Molecular Simulations Inc., Cambridge, UK (1995).
Davey, R. J., "Solvent Effects in Crystallization Processes," *Current Topics in Materials Science*, E. Kaldis, ed., North-Holland, Amsterdam, Vol. 8, p. 429 (1982).
Davey, R. J., B. Milisavljevic, and J. R. Bourne, "Solvent Interactions at Crystal Surfaces: The Kinetic Story of α-Resorcinol, " *J. Phys. Chem.*, **92**, 2032 (1988).
Davey, R. J., J. W. Mullin, and M. J. L. Whiting, "Habit Modification of Succinic Acid Crystals from Different Solvents, " *J. Cryst. Growth*, **58**, 304 (1982).
di Martino, P., A.-M. Guyot-Hermann, P. Conflant, M. Drache, and J.-C. Guyot, "A New Pure Paracetamol for Direct Compression: The Orthorhombic Form, " *Int. J. Pharm.*, **128**, 1 (1996).
Duverneuil, P., N. Hiquily, and R. Ousset, "A Comparison of the Effects of Some Solvents on the Growths of HMX (Octogene) Crystals from Solutions," *Proceedings of the 10th Symposium on Industrial Crystallization 1987*, J. Nyvlt and S. Zacek, eds., Elsevier Science, Amsterdam, p. 525 (1987).
Elwenspoek, M., P. Bennema, and J. P. van der Eerden, "Oriental Order in Naphthalene Crystal–Solution Interfaces," *J. Cryst. Growth*, **83**, 297 (1987).
Finnie, S., R. I. Ristic, J. N. Sherwood, and A. M. Zikic, "Characterization of Growth Behaviour of Small Paracetamol Crystals Grown from Pure Solution," *Trans. IChemE*, **74A**, 835 (1996).
Finnie, S., R. I. Ristic, J. N. Sherwood, and A. M. Zikic, "Morphological and Growth Rate Distributions of Small Self-Nucleated Paracetamol Crystals Grown from Pure Aqueous Solution," *J. Cryst. Growth*, **207**, 308 (1999).
Fletcher, R., *Sums of Squares and Nonlinear Equations, Practical Methods of Optimization*, 2nd Edition, Wiley, New York, p. 111 (1987).
Franks, F., *Water*, The Royal Society of Chemistry, London (1983).
Fredenslund, A., R. L. Jones, and J. M. Prausnitz, "Group-Contribution Estimation of Activity Coefficients in Nonideal Liquid Mixtures, " *AIChE J.*, **2**(6), 1086 (1975).
Gilmer, G. H., and P. Bennema, "Simulation of Crystal Growth with Surface Diffusion," *J. Appl. Phys.*, **43**(4), 1347 (1972).
Gilmer, G. H., and P. Bennema, "Computer Simulation of Crystal Surface and Growth Kinetics," *J. Cryst. Growth*, **13/14**, 148 (1972).
Gracin, S., T. Brink, and Å. C. Rasmuson, "Prediction of Solubility of Solid Organic Compounds in Solvents by UNIFAC," *Ind. Eng. Chem. Res.*, **41**, 5114 (2002).
Granberg, R. A., D. G. Bloch, and Å. C. Rasmuson, "Crystallization of Paracetamol in Acetone–Water Mixtures," *J. Cryst. Growth*, **198/199**, 1287 (1999).
Granberg, R. A., C. Ducreux, S. Gracin, and Å. C. Rasmuson, "Influence of Solvent Composition on Primary Nucleation of Paracetamol in Acetone–Water Mixtures, " *Chem. Eng. Sci.*, **56**, 2305 (2000).
Granberg, R. A., and Å. C. Rasmuson, "Crystallization of Paracetamol in Acetone–Toluene Mixtures, *Crystal Growth of Organic Materials 4* (CGOM4), J. Ulrich, ed., Shaker Verlag, Herzogenrath, Germany, p. 146 (1997).
Granberg, R. A., and Å. C. Rasmuson, "Solubility of Paracetamol in Pure Solvents," *J. Chem. Eng. Data*, **44**, 1391 (1999).
Granberg, R. A., and Å. C. Rasmuson, "Solubility of Paracetamol in Binary and Ternary Water + Acetone + Toluene Mixtures," *J. Chem. Eng. Data*, **45**, 478 (2000).
Grant, D. J. W., and A. H.-L. Chow, "Crystal Modifications in Acetaminophen by Growth from Aqueous Solutions Containing *p*-Acetoxyacetanilide, A Synthetic Impurity," *AIChE Symp. Ser.*, **87**(284), 33 (1991).
Grant, D. J. W., and T. Higuchi, "Solubility Behavior of Organic Compounds," *Techniques of Chemistry*, W. H. Sanders, Jr., ed., Wiley–Interscience, New York, Vol. 21 (1990).
Green, D. A., and P. Meenan, "Acetaminophen Crystal Habit: Solvent Effects," *CGOM 3*, A. S. Myerson, D. A. Green, and P. Meenan, eds., ACS Conference Proceedings Series, August 1995, Washington, DC, p. 78 (1996).
Haisa, M., S. Kashino, R. Kawai, and H. Maeda, "The Monoclinic Form of *p*-Hydroxyacetanilide, " *Acta Cryst.*, **B32**, 1283 (1976).
Haisa, M., S. Kashino, and H. Maeda, "The Orthorhombic Form of *p*-Hydroxyacetanilide," *Acta Cryst.*, **B30**, 2510 (1974).
Hansen, H. K., P. Rasmussen, and A. Fredeslund, "Vapor–Liquid Equilibria by UNIFAC Group Contribution. 5. Revision and Extension," *Ind. Eng. Chem. Res.*, **30**, 2352 (1991).
Hartman, P., and W. G. Perdok, "On the Relations between Structure and Morphology of Crystals, Part 1, " *Acta Cryst.*, **8**, 49 (1955a).
Hartman, P., and W. G. Perdok, "On the Relations between Structure and Morphology of Crystals, Part 2, " *Acta Cryst.*, **8**, 521 (1955b).
Hashim, M. A., M. Balasubramaniam, and A. Abdul-Hamid, "Acid Effects in Liquid–Liquid Equilibria," *Proceedings of the International Conference on Recent Advances in Chemical Engineering*, D. N. Saraf and D. T. Kunzru, eds., McGraw-Hill, New Dehli, p. 329 (1989).
Hendriksen, B. A., and D. J. W. Grant, "The Effect of Structurally Related Substances on the Nucleation Kinetics of Paracetamol (Acetaminophen)," *J. Cryst. Growth*, **156**, 252 (1995).
Hendriksen, B. A., D. J. W. Grant, P. Meenan, and D. A. Green, "Crystallization of Paracetamol (Acetaminophen) in the Presence of Structurally Related Substances," *J. Cryst. Growth*, **183**, 629 (1998).
Hildebrand, J. H., J. M. Prausnitz, and R. L. Scott, *Regular and Related Solutions*, van Nostrand Reinhold, New York (1970).
Hollenbeck, R. G., "Determination of Differential Heat of Solution in Real Solutions from Variation in Solubility with Temperature," *J. Pharm. Sci.*, **69**(10), 1241 (1980).
Human, H. J., J. P. van der Eerden, L. A. M. J. Jetten, and J. G. M. Odekerken, "On the Roughening Transition of Biphenyl: Transition of Faceted to Nonfaceted Growth of Biphenyl for Growth from Different Organic Solvents and Melt," *J. Cryst. Growth*, **51**, 589 (1981).
Huyskens, P. L., and M. C. Haulait-Pirson, "A New Expression for the Combinatorial Entropy of Mixing in Liquid Mixtures," *J. Mol. Liq.*, **31**, 135 (1985).
Jackson, K. A., *Liquid Metals and Solidification*, American Chemical Society for Metals, Cleveland, OH (1958).
Jetten, L. A. M. J., H. J. Human, P. Bennema, and J. P. van der Eerden, "On the Roughening Transition of Organic Crystals, Growing from Solution," *J. Cryst. Growth*, **68**, 503 (1984).
Jones, A. G., and J. W. Mullin, "Crystallization Kinetics of Potassium Sulphate in a Draft-Tube Agitated Vessel," *Trans. IChemE*, **51**, 302 (1973).
Klug, D. L., "The Influence of Impurities and Solvents on Crystallization," *Handbook of Industrial Crystallization*, A. S. Myerson, ed., Butterworth-Heinemann, Boston, MA, p. 65 (1993).
Krtalic, S., *Prediction of Paracetamol and Succinic Acid Solubility in Various Solvents with UNIFAC*, MS Thesis, Department of Chemical Engineering and Technology, Royal Institute of Technology, Stockholm, Sweden (1998).
Linford, R. G., "Surface Energy of Solids," *Chem. Soc. Rev.*, **1**, 445 (1972).

Matz, G., "Formfaktoren von kristallen bei der Kristallisation," *Chem. Technik*, **11**(19), 1157 (1982).
Mersmann, A., "Calculations of Interfacial Tensions," *J. Cryst. Growth*, **102**, 841 (1990).
Mersmann, A., "General Prediction of Statistically Mean Growth Rates of a Crystal Collective," *J. Cryst. Growth*, **147**, 181 (1995).
Mullin, J. W., *Crystallization*, 3rd Edition, Butterworth-Heinemann, Oxford, UK (1993).
Myerson, A. S., and R. Ginde, "Crystals, Crystal Growth, and Nucleation," *Handbook of Industrial Crystallization*, A. S. Myerson, ed., Butterworth-Heinemann, Boston, MA, p. 33 (1993).
Neau, S. H., S. V. Bhandarkar, and E. W. Hellmuth, "Differential Molar Heat Capacities to Test Ideal Solubility Estimations," *Pharm. Res.*, **14**(5), 601 (1997).
Neau, S. H., and D. R. Howard, "Partial Molal Volumes of *n*-Alkyl *p*-Aminobenzoates in Nonpolar Solvents," *Int. J. Pharm.*, **77**(2–3), 239 (1991).
Neumann, A. W., and J. K. Spelt, *Applied Surface Thermodynamics* (Surfactants Science Series), Vol. 63, Marcel Dekker, New York (1996).
Nielsen, A. E., "Electrolyte Crystal Growth Mechanism," *J. Cryst. Growth*, **67**, 289 (1984).
Nielsen, A. E., and O. Söhnel, "Interfacial Tensions, Electrolyte Crystal-Aqueous Solution, from Nucleation Data," *J. Cryst. Growth*, **11**, 233 (1971).
Nývlt, J., O. Söhnel, M. Matuchová, and M. Broul, *The Kinetics of Industrial Crystallization*, Elsevier, Amsterdam, p. 35 (1985).
Ohara, M., and R. C. Reid, *Modeling Crystal Growth Rates from Solution*, Prentice-Hall, Englewood Cliffs, NJ (1973).
Olech, A. Z., and S. A. Hodorowicz, "The Growth Kinetics of Urea Monocrystals from 1-Propanol-Aqueous Solution," *J. Cryst. Growth*, **102**, 562 (1990).
Prasad, K. V. R., R. I. Ristic, D. B. Sheen, and J. N. Sherwood, "Crystallization of Paracetamol from Pure and *p*-Acetoxyacetanilide (PAA) Doped Solutions," Proc. of 14th Symposium on Industrial Crystallization, IChemE, Rugby, UK (1999).
Prausnitz, J. M., R. N. Lichtentaler, and E. D. de Azevedo, *Molecular Thermodynamics of Fluid-Phase Equilibria*, Prentice-Hall, Upper Saddle River, NJ (1999).
Qiu, Y., and Å. C. Rasmuson, "Growth and Dissolution of Succinic Acid Crystals in a Batch Stirred Crystallizer," *AIChE J.*, **36**(5), 665 (1990).
Shekunov, B. Y., M. E. Aulton, R. W. Adama-Acquah, and D. J. W. Grant, "Effect of Temperature on Crystal Growth and Crystal Properties of Paracetamol," *J. Chem. Soc. Faraday Trans.*, **92**(3), 439 (1996).
Shekunov, B. Y., and D. J. W. Grant, "In Situ Optical Interferometric Studies of the Growth and Dissolution Behavior of Paracetamol (Acetaminophen). 1. Growth Kinetics," *J. Phys. Chem. B*, **101**, 3973 (1997).
Skoda, W., and M. van den Tempel, "Growth Kinetics of Triglyceride Crystals," *J. Cryst. Growth*, **1**, 207 (1967).
Sloan, G. J., and A. R. McGhie, *Techniques of Melt Crystallization*, Vol. 19, Wiley, New York (1988).
Snow, R. L., J. B. Ott, J. R. Goates, K. N. Marsh, S. O'Shea, and R. H. Stokes, "(Solid + Liquid) and (Vapor + Liquid) Phase Equilibria and Excess Enthalpies for (Benzene + *n*-Tetradecane), (Benzene + *n*-Hexadecane), (Cyclohexane + *n*-Tetradecane), and (Cyclohexane + *n*-Hexadecane) at 293.15, 298.15, and 308.15 K. Comparison of G_m^E Calculated from (Vapor + Liquid) and (Solid + Liquid) and Equilibria," *J. Chem. Thermodyn.*, **18**, 107 (1986).
Sohn, Y. T., "Study on the Polymorphism of Acetaminophen," *Kor. Pharm. Sci.*, **20**, 97 (1990).
Söhnel, O., and J. W. Mullin, "Interpretation of Crystallization Induction Periods," *J. Colloid Interface Sci.*, **123**(1), 43 (1988).
Stokes, R. J., and D. F. Evans, *Fundamentals of Interfacial Engineering*, Wiley–VCH, New York (1997).
Tanimoto, A., K. Kobayashi, and S. Fujita, "Overall Crystallization Rate of Copper Sulfate Pentahydrate in an Agitated Vessel," *Int. Chem. Eng.*, **4**(1), 153 (1964).
Temkin, D. E., *Crystallization Process*, Consultants Bureau, New York (1966).
Uusi-Penttilä, M. S., and Å. C. Rasmuson, "Experimental Study for Agglomeration Behaviour of Paracetamol in Acetone–Toluene–Water Systems, " *IChemE Trans. A—Chem. Eng. Res. Des.*, **81**, 489 (2003).
van Hoof, P. J. C. M., M. Schoutsen, and P. Bennema, "Solvent Effect on the Roughening and Wetting of *n*-Paraffin Crystals," *J. Cryst. Growth*, **192**, 307 (1998).
van Krevelen, D. W., "Interfacial Energy Properties," *Properties of Polymers*, Elsevier, Amsterdam, p. 227 (1990).
van Oss, C. J., "Acid–Base Interfacial Interactions in Aqueous Media," *Colloids Surf. A Physicochem. Eng Aspects*, **78**, 1 (1993).
von Nürnberg, E., and A. Hopp, "Studies on Paracetamol Concerning Its Pharmaceutical-Technological Properties: 1. Model Crystallization Experiments in an X-ray Diffractometer," *Pharm. Ind.*, **44**(10), 1081 (1982).
Walas, S. M., *Phase Equilibria in Chemical Engineering*, Butterworth, Stoneham, MA (1985).
Walton, J. H., and J. D. Jenkins, "A Study of the Ternary System, Toluene–Acetone–Water," *J. Am. Chem. Soc.*, **45**, 2555 (1923).
Welton, J. M., and G. J. McCarthy, "X-ray Powder Data for Acetaminophen," *Powder Diffr.*, **3**(2), 102 (1988).

Manuscript received Dec. 16, 2003, and revision received Dec. 22, 2004.